Supplementary figures and tables

High resilience of carbon transport in long-term drought stressed mature Norway spruce trees within two weeks after drought release

Kyohsuke Hikino, Jasmin Danzberger, Vincent P. Riedel, Romy Rehschuh, Nadine K. Ruehr, Benjamin D. Hesse, Marco M. Lehmann, Franz Buegger, Fabian Weikl, Karin Pritsch, Thorsten E. E. Grams

Supplementary figures

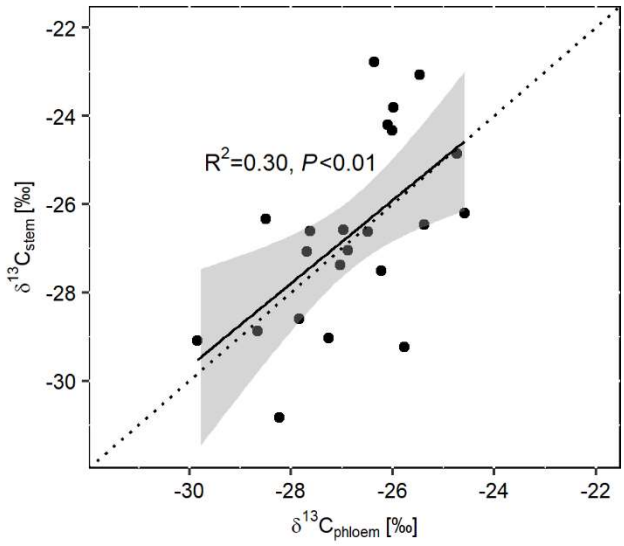

Figure S 1: Correlation between $\delta^{13}C$ of stem CO_2 efflux ($\delta^{13}C_{stem}$) and $\delta^{13}C$ of stem phloem sugar ($\delta^{13}C_{phloem}$). The dashed line is 1:1 line and the solid line is the calculated regression line (slope = 0.94). The gray area displays the 95% confidence interval.

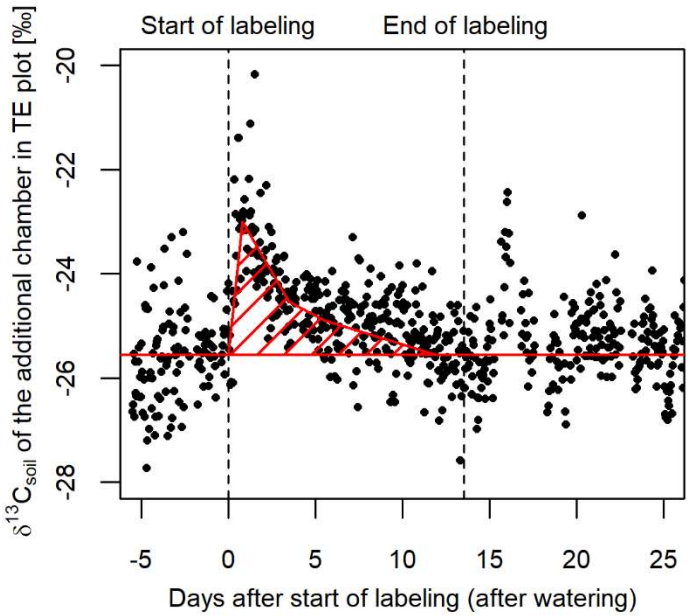

Figure S 2: $\delta^{13}C$ of the additional soil chamber ($\delta^{13}C_{soil}$) close to the non-labeled beech trees in the TE (previously drought-stressed, throughfall exclusion) plot (see Figure 2a). Dashed lines indicate start and end of labeling. The red horizontal line displays the mean $\delta^{13}C_{soil}$ before the start of labeling. The shift of $\delta^{13}C_{soil}$ after watering/start of labeling (roughly marked with red striped area for the first 12 days) was subtracted from the $\delta^{13}C_{soil}$ of the soil chambers under labeled trees in the TE plot (for details see Figure S3).

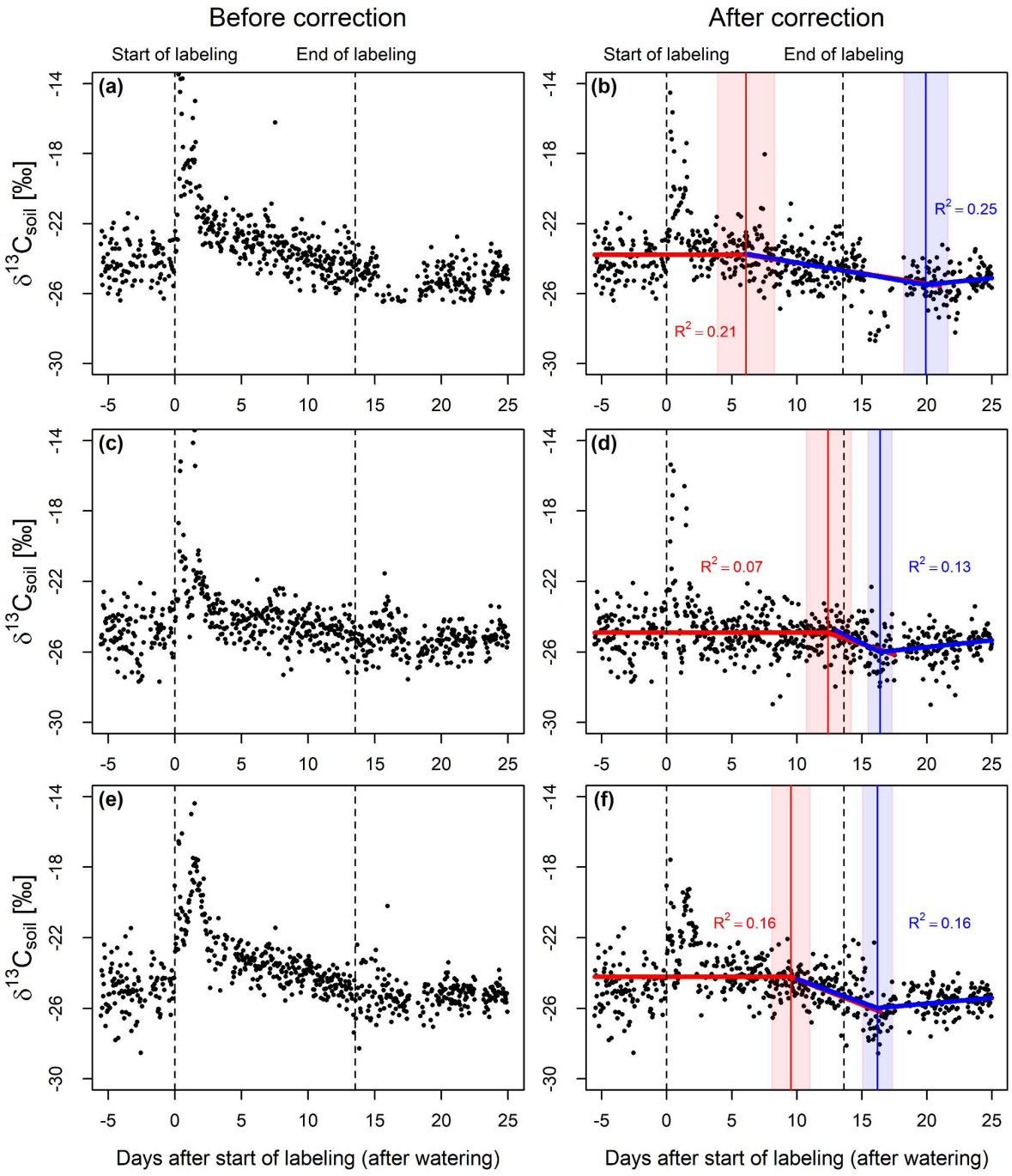

Figure S 3: The correction of $\delta^{13}C$ of soil CO_2 efflux ($\delta^{13}C_{soil}$) under labeled, previously drought-stressed trees (TE, throughfall exclusion, n = 3) using the additional soil chamber (see Figure S2): $\delta^{13}C_{soil}$ of three TE soil chamber before (a, c, e) and after the correction (b, d, f), respectively. The gap between the values before and after the watering (start of labeling) was properly corrected, enabling to calculate the arrival time of the tracers with piecewise functions. Dashed lines indicate the start and the end of the labeling period. The red and blue lines fitted to the data show the results of the piecewise functions (see Materials and Methods in the main document). The red and blue vertical lines give the calculated arrival time of ^{13}C-depleted (after turn-on of the CO_2 exposure) and unlabeled tracer (after turn-off of the CO_2 exposure), respectively. The red and blue shaded area show the 95% confidence interval of the intersections.

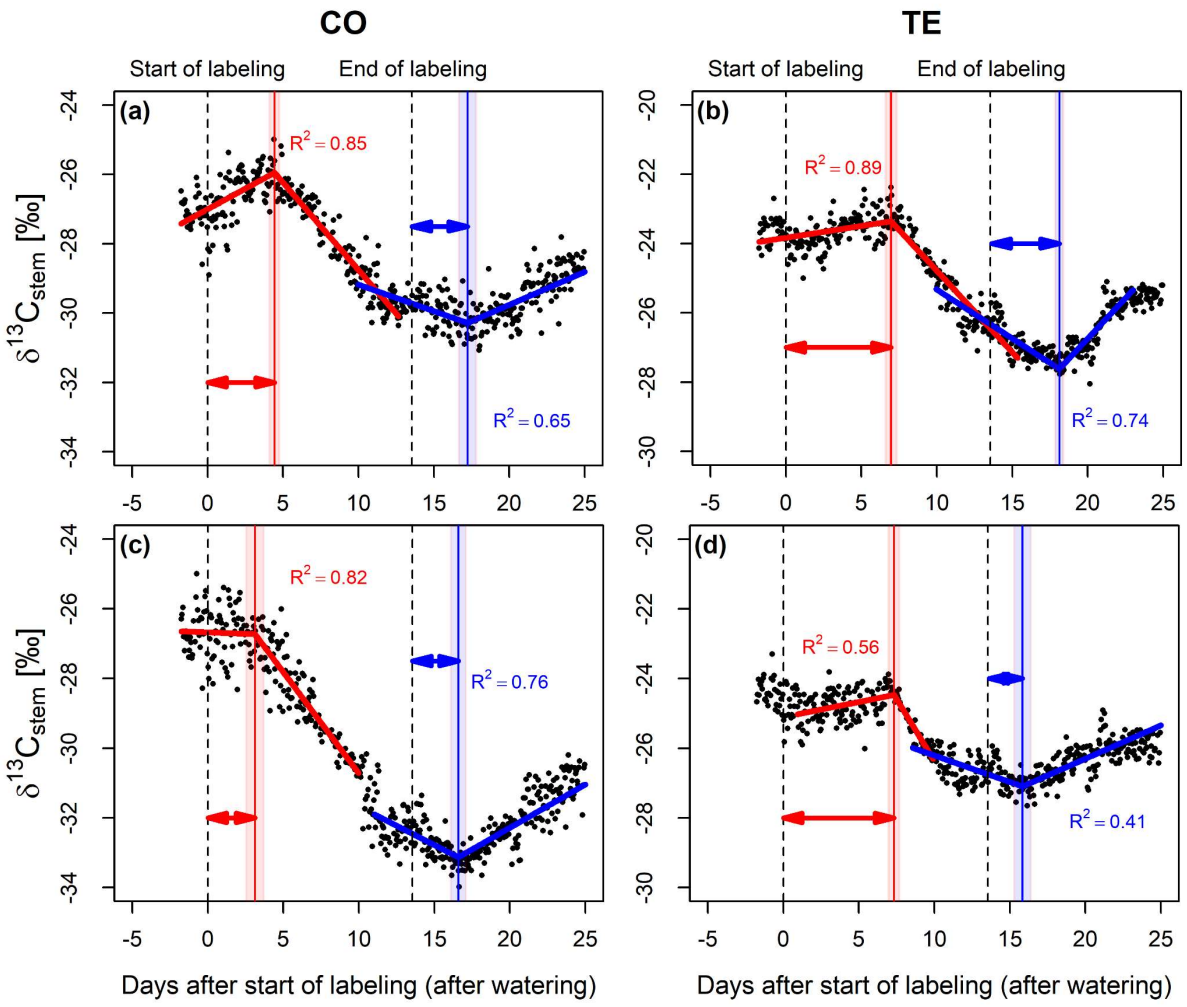

Figure S 4: The other data of $\delta^{13}C$ of stem CO_2 efflux ($\delta^{13}C_{stem}$) in CO (control, a, c) and TE (previously drought-stressed, throughfall exclusion, b,d) plots, used for the calculation of the arrival time of the ^{13}C-tracers (see Materials and Methods in the main document, Figure 4). Dashed vertical lines are the start and the end of labeling. The red and blue lines fitted to the data show the results of the piecewise functions to estimate the arrival time of ^{13}C-depleted and unlabeled tracer, respectively. The intersections of two lines, marked with solid red and blue vertical lines are the calculated arrival times in the first week and two weeks after the watering, respectively. These arrival times (displayed here with arrows) were then used to calculate the aboveground carbon transport rates (CTR_{above}). The red and blue shaded area give the 95% confidence interval of the intersections.

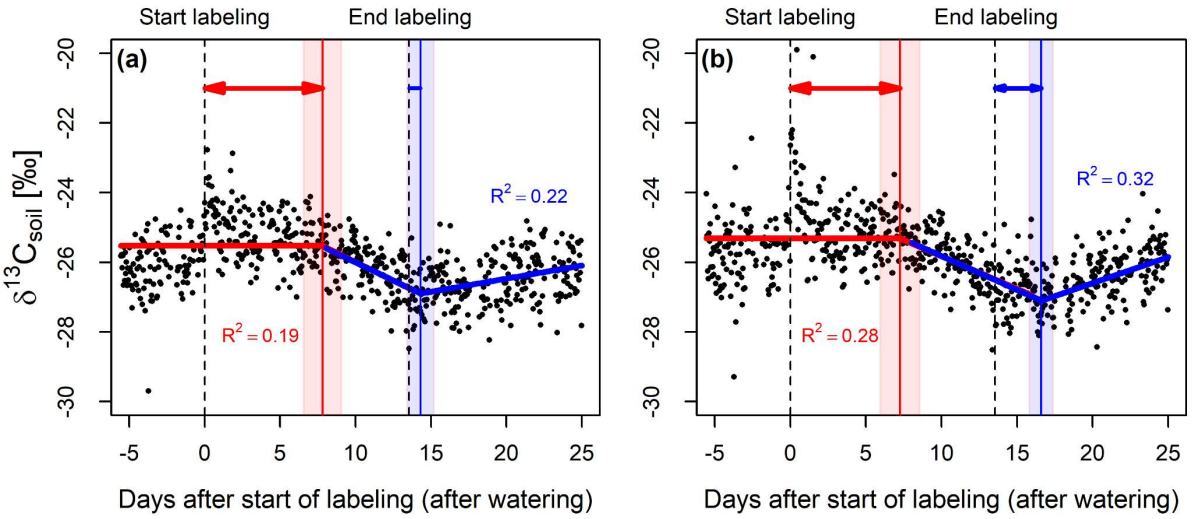

Figure S 5: The other data of $\delta^{13}C$ of soil CO_2 efflux ($\delta^{13}C_{soil}$) in CO (control) plot, used for the calculation of the arrival time of the ^{13}C-tracers (see Materials and Methods in the main document, Figure 4). Dashed vertical lines are the start and the end of labeling. The red and blue lines fitted to the data show the results of the piecewise functions to estimate the arrival time of ^{13}C-depleted and unlabeled tracer, respectively. The intersections of two lines, marked with solid red and blue vertical lines are the calculated arrival times in the first week and two weeks after the watering, respectively. These arrival times (displayed here with arrows) were then used to calculate the belowground carbon transport rates (CTR_{below}). The red and blue shaded area give the 95% confidence interval of the intersections.

Supplementary tables

Table S 1: Diameter at breast height (DBH), mean crown height (middle of the crown), and daily mean shift of CO_2 concentration and stable carbon isotope composition ($\delta^{13}C_a$) of canopy air during labeling hours (5 am – 7 pm CET) of four labeled control (CO) and three labeled thoughfall exclusion (TE, previously drought stressed) trees. Shifts are given in means ± SE. The fourth tree on the CO plot was not the object of the calculation of arrival time and C transport rates (CTR), therefore, its mean crown height was not measured.

	DBH [cm]	Mean crown height [m]	Shift of CO_2 concentration [ppm]	Shift of $\delta^{13}C_a$ [‰]
CO_1	30.5	28.6	111 ± 8	-6.7 ± 0.4
CO_2	34.9	27.9	112 ± 8	-6.7 ± 0.4
CO_3	46.3	28.7	119 ± 8	-7.2 ± 0.4
CO_4	37.7	-	162 ± 10	-8.8 ± 0.4
TE_1	45.1	27.3	72 ± 5	-5.0 ± 0.3
TE_2	27.3	25.4	132 ± 8	-7.3 ± 0.4
TE_3	38.3	28.4	35 ± 5	-2.9 ± 0.3

Table S 2: Number of trees and sampling positions assessed for this study in labeled and non-labeled plots in each treatment: i.e. control (CO) and throughfall exclusion (TE, previously drought stressed). n.a.= not assessed. A_{sat} (light-saturated CO_2 assimilation rates), Ψ_{PD} (Pre-dawn leaf water potential), π_O (leaf osmotic potential).

Number of trees/ sampling positions	Labeled		Non-labeled	
	CO	TE	CO	TE
Spruce tree	4	3	3	3
Canopy air	7	6	1	1
Stem CO_2 efflux	3	3	3	3
Soil CO_2 efflux	3	3	n.a.	1
Root tips	18	17	11	5
Stem phloem	4	3	n.a.	n.a.
A_{sat}, Ψ_{PD}, π_O	2	2	4	4

Table S 3: Days of sampling/assessment of each parameter (days marked in gray are the timing of assessments). A_{sat} (light-saturated CO_2 assimilation rates), Ψ_{PD} (Pre-dawn leaf water potential), π_O (leaf osmotic potential).

Days respective to watering/ start of labeling	-14	-7	-6	...	-2	-1	0	1	2	3	4	5	6	7	...	13	14	15	16	17	18	19	20	21	22	23	24	25
Stem CO_2 efflux																												
Soil CO_2 efflux																												
Root tips																												
Stem phloem																												
A_{sat}																												
Ψ_{PD}																												
π_O																												